

Mitigation of the Harmonics under Reactive Power Compensation by SHPF-TCR Using PI & Fuzzy Logic Technique

B. Aishwarya*, N. Swathi**

*P.G Student, Department of EEE, DIET College of Engineering, Visakhapatnam-531002

**Associate Professor, Department of EEE, DIET College of Engineering, Visakhapatnam-531002

ABSTRACT

In this paper, a combined system of a thyristor-controlled reactor (TCR) and a shunt hybrid power filter (SHPF) has been designed by MATLAB/SIMULINK approach for harmonic and reactive power compensation. The quality of the power is effected by many factors like harmonic contamination, due to the increment of non-linear loads, sag and swell due to the switching of the loads etc. Also control schemes based on PI and Fuzzy logic controllers have been proposed to mitigate the harmonics and neutral current. The proposed methodology not only reduces the complexity but also offers simplicity to implement and increases reliability of the system. These control strategies also help in achieving a low cost highly effective control. The performance is also observed under influence of utility side disturbances such as harmonics, flicker and spikes with Non-Linear and Reactive Loads with different control strategies.

Keywords: Harmonic suppression, Hybrid power filter, modeling, non linear control, reactive power compensation, Shunt Hybrid Power Filter and Thyristor Controlled Reactor (SHPF-TCR compensator), thyristor-controlled reactor (TCR), Fuzzy logic Controller.

I. INTRODUCTION

The quality of electrical power is one of the major growing concerns for utility as well as consumers. The increasing use of non linear and poor power factor loads such as Power electronic converters, Arc furnace, Adjustable speed, uninterruptable power supplies etc. are the responsible factor for the power quality issues. The most important factors of poor power quality are harmonics and high neutral current. Poor power quality factors such as switching phenomena results in oscillatory transients in the electrical supply, connection of high power non-linear loads contributes to the generation of current and voltage harmonic components, voltage sags are generated due to the high economical losses, short-term voltage drops (sags) can trip electrical drives or more sensitive equipment, leading to costly interruptions of production etc[1]. The definition of power quality given in the IEEE dictionary originates in IEEE Std 1100: Power quality is the concept of powering and grounding sensitive equipment in a manner that is suitable to the operation of that equipment. Power quality problems are common in most of commercial, industrial and utility networks. Natural phenomena, such as lightning are the most frequent cause of power quality problems. Also, the connection of high power non-linear loads contributes to the generation of current and voltage harmonic components the most significant and critical power quality problems are voltage sags due to the high economical losses that can be generated. For all these reasons, from the

consumer point of view, power quality issues will become an increasingly important factor to consider in order satisfying good productivity. On the other hand, for the electrical supply industry, the quality of power delivered will be one of the distinguishing factors for ensuring customer loyalty in this very competitive and deregulated market. Reactive power, Power factor, Harmonic distortion and Voltage unbalance in power supply are the most important factors effecting power quality. According to IEEE-519, total harmonics distortion is defined as the summation of the effective value of the harmonics components in the distorted waveform relative to the fundamental component. It can be calculated for either voltage or current. To reduce the Total Harmonic Distortion (THD) the basic principles are (a) Reduce the harmonic currents produced by the load. (b) Add filters to remove the harmonic currents off the system, block the currents from entering the system, or supply the harmonic currents locally. (c) Modify the frequency response of the system by filters, inductors, or capacitors. Vital use of power electronic appliances has made power management smart, flexible and efficient. But side by side they are leading to power pollution due to the injection of current and voltage harmonics. Traditionally, Passive filter have been used for mitigating the distortion due to harmonic current in industrial power systems. But they have many drawbacks such as resonance problem, dependency of their performance on the system impedance, absorption of harmonic current of nonlinear load,

which could lead to further harmonic propagation through the power system [2]. To overcome of such problem active power filters is introduced. It has no such drawbacks like passive filter. They inject harmonic voltage or current with appropriate magnitudes and phase angle into the system and cancel harmonics of nonlinear loads. But it has also some drawbacks like high initial cost and high power losses due to which it limits there wide application, especially with high power rating system. [3]–[5]. They are more effective in harmonic compensation and have good performance [6]–[8]. However, the costs of active filters are relatively high for large-scale system and require high power converter ratings [9], [10]. To minimize these limitations, hybrid power filter have been introduced and implemented in practical system applications. Shunt hybrid filter consists of an active filter which is connected in series with the passive filter and with a three phase PWM inverter. This filter effectively mitigates the problem of a passive and active filter. It provides cost effective harmonic compensation, particularly for high power nonlinear loads. Hybrid filters effectively soften the problems of the passive filter and an active filter solution and provide cost-effective harmonic compensation, particularly for high-power nonlinear loads [11]–[14]. Many control techniques such as instantaneous reactive power theory, synchronous rotating reference frame, neural network techniques, nonlinear control [15], feedforward control [16], Lyapunov-function-based control [17], etc., have been used to improve the performance of the active and hybrid filters. Several filter topologies for compensating harmonics and reactive power have been reported in the literature [18]–[21]. In [20], a combination of a thyristor-controlled reactor (TCR) and a resonant impedance-type hybrid APF for harmonic cancellation, load balancing, and reactive power compensation has been proposed. The control strategy of the system is based on the voltage vector transformation for compensating the negative-sequence current caused by the unbalance load without using phase-locked loops. A predictive current controller based on the Smith predictor is proposed to compensate the generalized current delay. A combined system of a static var compensator (SVC) and a small-rated APF for harmonic suppression and reactive power compensation has been reported in [21]. In this paper, a new combination of a shunt hybrid power filter (SHPF) and a TCR (SHPF-TCR compensator) is proposed to suppress current harmonics and compensate the reactive power generated from the load. The hybrid filter consists of a series connection of a small-rated active filter and a fifth-tuned LC passive filter. In the proposed

topology, the major part of a three-phase full-bridge voltage-source pulse width modulation (PWM) inverter with an input boost inductor (L_{pf}, R_{pf}) and a dc bus capacitor (C_{dc}). The APF sustains very low fundamental voltages and currents of the power grid, and thus, its rated capacity is greatly reduced. Because of these merits, the presented combined topology is very appropriate in compensating reactive power and eliminating harmonic currents in power system. This work study the compensation principle and different control strategies used here are based on PI/FUZZY controller of the shunt and TCR active filter in detail. The control strategies are modeled using MATLAB/SIMULINK. The performance is also observed under influence of utility side disturbances such as harmonics, flicker and spikes with Non-Linear and Reactive Loads. The simulation results are listed in comparison of different control strategies and for the verification of results.

II. SYSTEM CONFIGURATION OF SHPF-TCR COMPENSATOR.

Fig. 1 shows the topology of the proposed combined SHPF and TCR. The SHPF consists of a small-rating APF connected in series with a fifth-tuned LC passive filter. The APF consists of a three-phase full-bridge voltage-source pulse width modulation (PWM) inverter with an input boost inductor (L_{pf}, R_{pf}) and a dc bus capacitor (C_{dc}). Shunt active power filter compensate current harmonics by injecting equal-but-opposite harmonic compensating current. In this case the shunt active power filter operates as a current source injecting the harmonic components generated by the load but phase shifted by 180 degrees. This principle is applicable to any type of load considered a harmonic source. Moreover, with an appropriate control scheme, the active power filter can also compensate the load power factor. Because of these merits, the presented combined topology is very appropriate in compensating reactive power and eliminating harmonic currents in power system. The tuned passive filter in parallel with TCR forms a shunt passive filter (SPF). This is the most commonly used configuration of passive filters. This passive filter scheme helps in sinking the more dominant 5th and 7th and other higher order harmonics and thus prevents them from flowing into ac mains and PF correction. The small-rating APF is used to filter harmonics generated by the load and the TCR by enhancing the compensation characteristics of the SPF aside from eliminating the risk of resonance between the grid and the SPF. The TCR goal is to obtain a regulation of reactive power.

A. Mathematical modeling of SHPF

The system equations are first elaborated in abc reference frame. Using Kirchoff's voltage and current laws provides three differential equations in the stationary "a-b-c" frame (for k = 1, 2, 3).

$$V_{SK} = L_{PF} \frac{di_{ck}}{dt} + R_{PF} i_{ck} + \frac{1}{C_{PF}} \int i_{ck} dt + v_{kM} + v_{MN} \dots\dots\dots(1)$$

On differentiating (1) we get

$$\frac{dv_{sk}}{dt} = L_{PF} \frac{d^2 i_{ck}}{dt^2} + R_{PF} \frac{di_{ck}}{dt} + \frac{1}{C_{PF}} i_{ck} + \frac{dv_{kM}}{dt} + \frac{dv_{MN}}{dt} \dots\dots (2)$$

Assume that the zero sequence current is absent in a three phase system and the source voltages are balanced, so we obtain:

$$v_{MN} = \frac{-1}{3} \sum_{k=1}^3 v_{kM} \dots\dots\dots(3)$$

We can define the switching function C_k of the converter k_{th} leg as being the binary state of the two switches S_k and S_k^1 . Hence, the switching C_k (for k = 1, 2, 3) is defined as

$$C_k = 1, \text{ if } S_k \text{ is on and } S_k^1 \text{ is off} \\ C_k = 0, \text{ if } S_k \text{ is off and } S_k^1 \text{ is on} \dots\dots\dots(4)$$

Thus, with $V_{kM} = C_k V_{dc}$, and from (4), the following relation is obtained:

$$\frac{d^2 i_{ck}}{dt^2} = -\frac{R_{PF}}{L_{PF}} \frac{di_{ck}}{dt} - \frac{1}{C_{PF} L_{PF}} i_{ck} - \frac{1}{L_{PF}} (C_k - \frac{1}{3} \sum_{m=1}^3 C_m) \dots\dots\dots(5)$$

Let the switching state function be defined as

$$q_{nk} = (C_k - \frac{1}{3} \sum_{m=1}^3 C_m) n \dots\dots\dots(6)$$

Hence we got the relation as

$$\begin{bmatrix} q_{n1} \\ q_{n2} \\ q_{n3} \end{bmatrix} = \frac{1}{3} \begin{bmatrix} 2 & -1 & -1 \\ -1 & 2 & -1 \\ -1 & -1 & 2 \end{bmatrix} \begin{bmatrix} C_1 \\ C_2 \\ C_3 \end{bmatrix} \dots\dots\dots(7)$$

Hence the complete model of the active filter in "a-b-c" reference frame is obtained as follows

$$L_{PF} \frac{d^2 i_{c1}}{dt^2} = -R_{PF} \frac{di_{c1}}{dt} - \frac{1}{C_{PF}} i_{c1} - q_{n1} \frac{dv_{dc}}{dt} + \frac{dv_{s1}}{dt} \\ L_{PF} \frac{d^2 i_{c2}}{dt^2} = -R_{PF} \frac{di_{c2}}{dt} - \frac{1}{C_{PF}} i_{c2} - q_{n2} \frac{dv_{dc}}{dt} + \frac{dv_{s2}}{dt} \\ C_{dc} \frac{dv_{dc}}{dt} = (2q_{n1} + q_{n2}) i_{c1} + (q_{n1} + 2q_{n2}) i_{c2} \dots\dots\dots(8)$$

The above model is time varying and nonlinear in nature. Then, by applying d-q transformation.

This model is nonlinear because of the existence of multiplication terms between the state variables $\{i_d, i_q, V_{dc}\}$ and the switching state function $\{d_{nd}, d_{nq}\}$. The complete model in the d-q frame is

$$L_{PF} \frac{d^2 i_d}{dt^2} = -R_{PF} \frac{di_d}{dt} + 2\omega L_{PF} \frac{di_d}{dt} - (-\omega^2 L_{PF} + \frac{1}{C_{PF}}) i_d \\ + \omega R_{PF} i_q - q_{nd} \frac{dv_{dc}}{dt} + \frac{dv_d}{dt} - \omega v_q \\ L_{PF} \frac{d^2 i_q}{dt^2} = -R_{PF} \frac{di_q}{dt} - 2\omega L_{PF} \frac{di_q}{dt} - (-\omega^2 L_{PF} + \frac{1}{C_{PF}}) i_q \\ - \omega R_{PF} i_d - q_{nq} \frac{dv_{dc}}{dt} + \frac{dv_q}{dt} + \omega v_d \\ C_{dc} \frac{dv_{dc}}{dt} = q_{nd} i_d + q_{nq} i_q \dots\dots\dots(9)$$

However, the model is time invariant during a given switching state. Furthermore, the principle of operation of the SHPF requires that the three state variables have to be controlled independently. The interaction between the inner current loop and the outer dc bus voltage loop can be avoided by adequately separating their respective dynamics. Since the steady state fundamental components are sinusoidal, the system is transformed into the d-q reference frame at constant supply frequency. The conversion matrix is

$$C_{dq}^{123} = \sqrt{\frac{2}{3}} \begin{bmatrix} \cos \theta & \cos(\theta - 2\pi/3) & \cos(\theta - 4\pi/3) \\ -\sin \theta & -\sin(\theta - 2\pi/3) & -\sin(\theta - 4\pi/3) \end{bmatrix} \dots\dots\dots(10)$$

where $\theta = \omega t$, and the following equalities hold

$$C_{123}^{dq} = (C_{dq}^{123})^{-1} = (C_{dq}^{123})^T$$

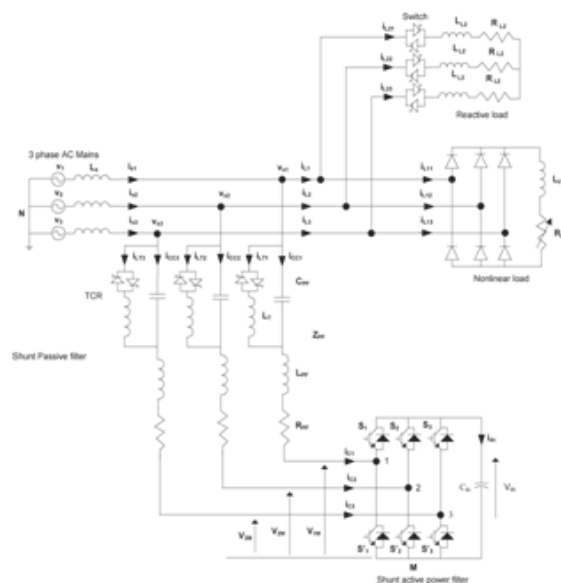


Fig.1.Basic circuit of the proposed SHPF-TCR compensator.

B. Harmonic Current Control.

$$L_{PF} \frac{d^2 i_d}{dt^2} + R_{PF} \frac{di_d}{dt} + (-\omega^2 L_{PF} + \frac{1}{C_{PF}}) i_d = 2\omega L_{PF} \frac{di_q}{dt} + \omega R_{PF} i_q - q_{nd} \frac{dv_{dc}}{dt} + \frac{dv_d}{dt} - \omega v_q \dots(11)$$

$$L_{PF} \frac{d^2 i_q}{dt^2} - R_{PF} \frac{di_q}{dt} + (-\omega^2 L_{PF} + \frac{1}{C_{PF}}) i_q = -2\omega L_{PF} \frac{di_d}{dt} + \omega R_{PF} i_d - q_{nq} \frac{dv_{dc}}{dt} + \frac{dv_q}{dt} - \omega v_d \dots(12)$$

$$u_d = 2\omega L_{PF} \frac{di_q}{dt} + \omega R_{PF} i_q - q_{nd} \frac{dv_{dc}}{dt} + \frac{dv_d}{dt} - \omega v_q \dots(13)$$

$$u_q = -2\omega L_{PF} \frac{di_d}{dt} - \omega R_{PF} i_d - q_{nq} \frac{dv_{dc}}{dt} + \frac{dv_q}{dt} + \omega v_d \dots(14)$$

Now the TF of the model is

$$\frac{I_d(s)}{U_d(s)} = \frac{1}{L_{PF} s^2 + R_{PF}(s) + \frac{1}{C_{PF}} - L_{PF} \omega^2} \dots(15)$$

Transfer function of the PI controller is given as

$$G_i(s) = \frac{U_d(s)}{I_d(s)} = \frac{U_q(s)}{I_q(s)} = k_p + \frac{k_i}{s}$$

The closed loop transfer function of the current loop is

$$\frac{I_q(s)}{I_q^1(s)} = \frac{I_d(s)}{I_d^1(s)} = \frac{k_p}{L_{PF} s^3 + \frac{R_{PF}}{L_{PF}} s^2 + (\frac{1}{C_{PF} L_{PF}} - \omega^2 + \frac{k_p}{L_{PF}}) s + \frac{k_i}{L_{PF}}}$$

The control loop of the current iq is shown in the fig. below and the control law is

$$q_{nd} = \frac{2\omega L_{PF} \frac{di_q}{dt} + \omega R_{PF} i_q + \frac{dv_d}{dt} - \omega v_q - u_d}{\frac{dv_{dc}}{dt}}$$

$$q_{nq} = \frac{2\omega L_{PF} \frac{di_d}{dt} + \omega R_{PF} i_d + \frac{dv_q}{dt} - \omega v_d - u_q}{\frac{dv_{dc}}{dt}}$$

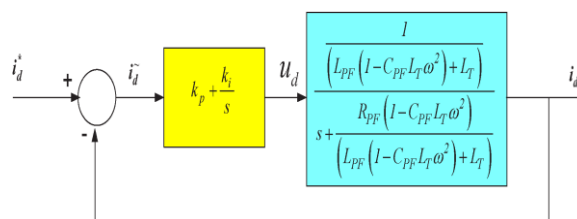


Fig. 2. Inner control loop of the current i_d .

C. DC Bus Voltage Regulation

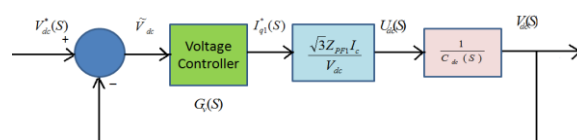


Fig. 3. Compensated voltage regulated model

The active filter produces a fundamental voltage which is in-phase with fundamental leading current of the passive filter. A small amount of active power is formed due to the leading current and fundamental voltage of the passive filter and it delivers to the dc capacitor. Therefore, the electrical quantity adjusted by the dc-voltage controller is consequently i_{q1}^* . To

maintain v_{dc} equal to its reference value, the losses through the active filter's resistive-inductive branches will be compensated by acting on the supply current. Eqn(9) can be rewritten as

$$C_{dc} \frac{dv_{dc}}{dt} = q_{nq} i_q \dots(16)$$

The three-phase filter currents are given by

$$\begin{bmatrix} i_{c1} \\ i_{c2} \\ i_{c3} \end{bmatrix} = \sqrt{\frac{2}{3}} i_q \begin{bmatrix} -\sin \theta \\ -\sin(\theta - \frac{2\Pi}{3}) \\ -\sin(\theta - \frac{4\Pi}{3}) \end{bmatrix} \dots(17)$$

The fundamental filter rms current I_c is given by

$$I_c = \frac{i_q}{\sqrt{3}} \dots(18)$$

the q axes active filter voltage v_{Mq} is given by

$$v_{Mq} = -Z_{PF1} i_{q1}^* \dots(19)$$

where Z_{PF1} is the impedance of the passive filter at 60 Hz and i_{q1}^* is a dc component.

An equivalent input u_{dc} is defined as

$$u_{dc} = q_{nq} i_q \dots(20)$$

The control effort of the dc-voltage loop is

$$i_{q1}^* = \frac{v_{dc}}{-Z_{PF1} i_q} u_{dc} \dots\dots(21)$$

The outer control loop of the dc voltage is shown in Fig(3). To regulate dc voltage v_{dc} , the error $\tilde{v}_{dc} = v_{dc}^* - v_{dc}$ is passing through a P-I type controller given by

$$u_{dc} = k_1 \tilde{v}_{dc} + k_2 \int \tilde{v}_{dc} dt \dots\dots(22)$$

Hence the closed loop transfer function of the fig is

$$\frac{v_{dc}(s)}{v_{dc}^*(s)} = \frac{\frac{v_{dc} C_{dc}}{s^2 + \frac{\sqrt{3}Z_{PF1}k_1 I_c}{v_{dc} C_{dc}}(s) + \frac{\sqrt{3}Z_{PF1}k_2 I_c}{v_{dc} C_{dc}}}}{\frac{v_{dc} C_{dc}}{s^2 + \frac{\sqrt{3}Z_{PF1}k_1 I_c}{v_{dc} C_{dc}}(s) + \frac{\sqrt{3}Z_{PF1}k_2 I_c}{v_{dc} C_{dc}}}} \dots\dots(23)$$

The proportional k_1 and integral k_2 gains are then obtained as

$$k_1 = 2\xi\omega_{nv} \left(\frac{v_{dc} C_{dc}}{\sqrt{3}Z_{PF1} I_c} \right) \dots\dots(24)$$

$$k_2 = \omega_{nv}^2 \left(\frac{v_{dc} C_{dc}}{\sqrt{3}Z_{PF1} I_c} \right)$$

By designing the dc bus voltage loop much slower than the current one, there would not be any interaction between the two loops. The proposed nonlinear controller of the proposed SHPF-TCR compensator is shown in Fig. 4.

D. Modelling of TCR

The susceptance is given by

$$B(\alpha) = B2\alpha - 2a + \sin(2\alpha) / \Pi \dots (25)$$

where $B = 1/LPF\omega$.

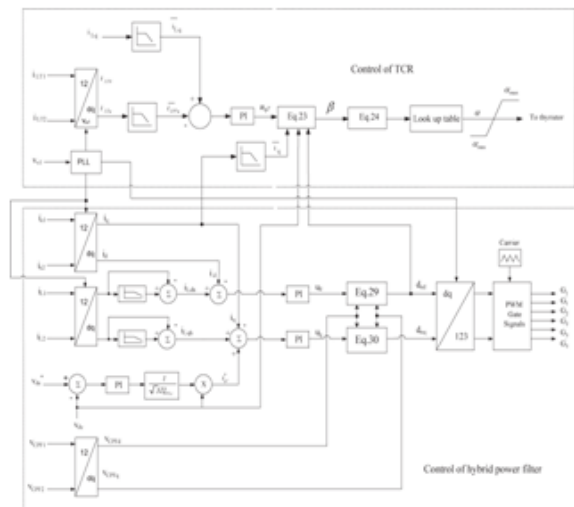


Fig. 4. Control scheme of the proposed SHPF-TCR compensator.

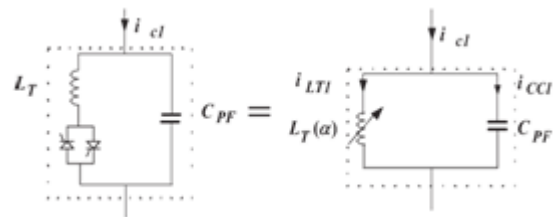


Fig.5: TCR equivalent circuit.

Fig. 6 illustrates the susceptance versus firing angle. A PI controller is used to force the reactive current of the SHPF-TCR compensator to follow exactly the reactive current consumed by the load.

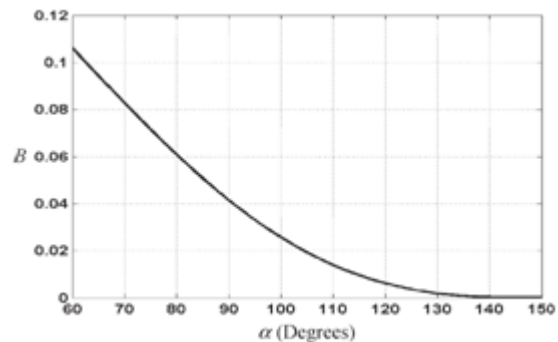


Fig. 6. Susceptance versus firing angle.

III. SHPF-TCR COMPENSATOR WITH PI CONTROLLER

PI control With a view to have a self-regulated dc bus, the voltage across the capacitor is sensed at regular intervals and controlled by employing a suitable closed loop control. The dc link voltage, vdc is sensed at a regular interval and is compared with its reference counterpart v_{dc}^* . The error signal is processed in a PI controller. The output of the PI controller is denoted as $i_{sp(n)}$. A limit is put on the output of controller this ensures that the source supplies active power of the load and dc bus of the SHPF-TCR Later part of active power supplied by source is used to provide a self-supported dc link of the SHPF-TCR Thus, the dc bus voltage of the SHPF-TCR is maintained to have a proper current control.

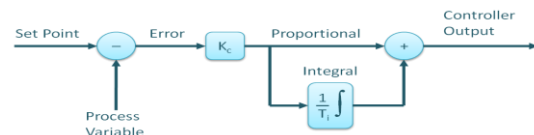


Fig.7: PI controller block with system

By using this PI Controller in the control scheme of the proposed SHPF-TCR compensator it has been shown that the system has a fast dynamic response, has good performance in both steady-state and transient operations, and is able to reduce the THD of supply currents well below the limit of 5% of the IEEE-519 standard. According to Haines, PI

control is the preferred method to improve the power quality because of the improvements in accuracy and energy consumption when compared to proportional control. A PI controller is a kind of linear controller, as it composes the control error according to the setting value and process output and then makes the controller output value based on the linear resultant of the error's proportion and integral. For a PI controller, the control signal at time t is

$$u(t) = K_p e(t) + K_i \int_0^t e(t) dt + u_o$$

where u(t) is the controller output, u_o is the controller initial output, K_p is the proportion parameter, K_i is the integral parameter, e(t) is the error at time t defined as $e(t) = y_{sp}(t) - y(t)$, where y_{sp} is the set point for process output at time t and y(t) is process output at time t. The transfer function of the PI controller is as follows:

$$G_e(s) = U(s) / E(s) = K_p + K_i / s$$

IV. SHPF-TCR COMPENSATOR WITH FUZZY CONTROLLER

The word Fuzzy means vagueness. Fuzziness occurs when the boundary of piece of information is not clear-cut. In 1965 Lotfi A. Zahed propounded the fuzzy set theory. Fuzzy set theory exhibits immense potential for effective solving of the uncertainty in the problem. Fuzzy set theory is an excellent mathematical tool to handle the uncertainty arising due to vagueness. Understanding human speech and recognizing handwritten characters are some common instances where fuzziness manifests. Fuzzy set theory is an extension of classical set theory where elements have varying degrees of membership. Fuzzy logic uses the whole interval between 0 and 1 to describe human reasoning. In FLC the input variables are mapped by sets of membership functions and these are called as "FUZZY SETS".

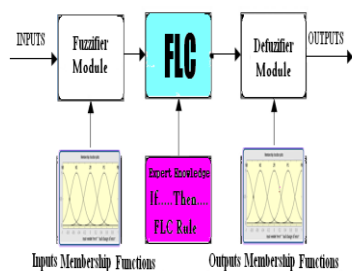


Fig.8 Fuzzy Basic Module

There are two major types of Fuzzy Rule Based Systems. They are (i) Mamdani Fuzzy Rule Based Systems and (ii) Takagi-Sugeno-Kang Fuzzy Rule Based Systems. Among the above Mamdani Fuzzy Rule Based Systems are more widely used in the industry.

A. Mamdani Fuzzy Rule – Based Systems These are the Fuzzy Rule Based Systems with fuzzifier and defuzzifier, more commonly these are known as Fuzzy Logic Controllers (FLC). The major constituents of the Mamdani Fuzzy Logic Controllers are shown in fig below.

Knowledge Base: The Knowledge Base (KB) stores the available knowledge about the problem in the form of fuzzy "IF THEN" rules. It composed of two main components, Data Base (DB) and Rule Base (RB). Data Base (DB) stores the membership functions of fuzzy sets and scaling functions for context adaptation purpose. Rule Base (RB) stores the FUZZY IF THEN rules for the purpose inference and decision making. Multiple rules can be fired simultaneously for the same input.

Fuzzification Interface: It transforms the crisp input data into fuzzy values that acts as input to fuzzy reasoning process.

Inference System: It infers from the fuzzy input to several resulting output fuzzy sets according to the information stored in the Knowledge Base (KB).

Defuzzification Interface: It converts the fuzzy sets obtained from the inference process into a crisp action that constitutes the global output of the FRBS. Mamdani based fuzzy logic interfacing rule is adopted for correction of power factor. Complex power is taken from power measuring block, in which power angle is taken as input of fuzzy controller. According to power angle control output (firing angle) is provided by fuzzy controller. When power angle is large firing angle is also large. Controlled output is supplied to thyristor. According to the output of variable time delay circuit firing angle of thyristor is changed. When power angle is very small then firing angle is also very small. When power angle is medium then firing angle is also medium. When power angle is large then firing angle is also large.

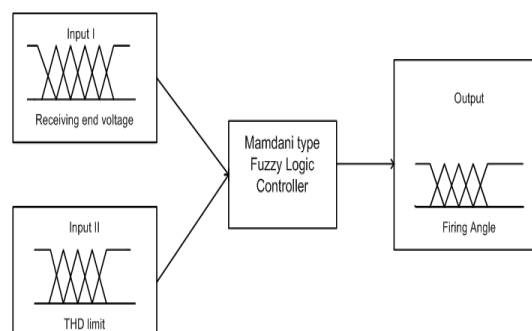


Fig.9 Flowchart used for implementation of fuzzy logic.

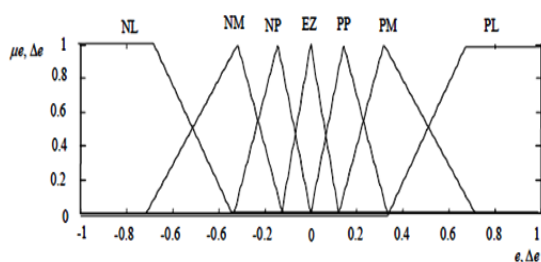


Fig.10. Membership functions for Input, Change in input, Output.

Rule Base: the elements of this rule base table are determined based on the theory that in the transient state, large errors need coarse control, which requires coarse in-put/output variables; in the steady state, small errors need fine control, which requires fine input/output variables. Based on this the elements of the rule table are obtained as shown in Table -I, with ‘Vdc’ and ‘Vdc-ref’ as inputs.

Table-I

e \ Δe	NL	NM	NS	EZ	PS	PM	PL
NL	NL	NL	NL	NL	NM	NS	EZ
NM	NL	NL	NL	NM	NS	EZ	PS
NS	NL	NL	NM	NS	EZ	PS	PM
EZ	NL	NM	NS	EZ	PS	PM	PL
PS	NM	NS	EZ	PS	PM	PL	PL
PM	NS	EZ	PS	PM	PL	PL	PL
PL	NL	NM	NS	EZ	PS	PM	PL

V. SIMULATION RESULTS

Simulations were performed numerically using the “Power System Blockset” simulator operating under Matlab/Simulink environment, in order to verify the operation of the proposed SHPF-TCR. Here simulation is carried out in several cases, in that 1). Proposed Hybrid Power Filter with Steady State & Transient Performances operated under PI Controller, 2). Proposed Hybrid Power Filter Operated under Fuzzy Controller.

Case 1: Proposed Hybrid Power Filter with Steady State & Transient Performances operated under PI Controller

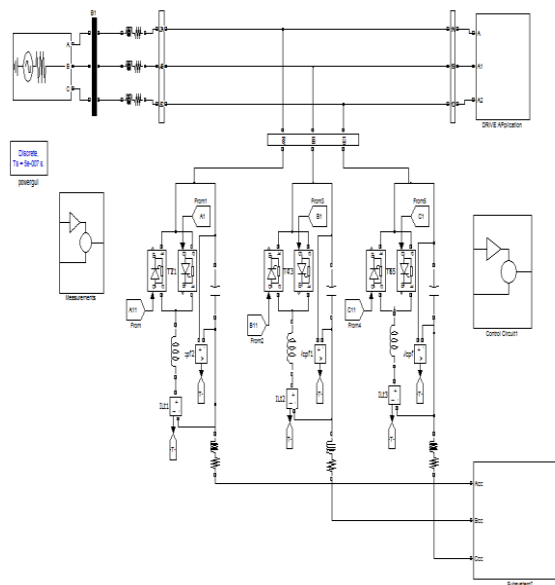


Fig.11 Matlab/Simulink Model of Proposed Shunt Hybrid Filter with TCR Combination for Enhancing PQfeatures

Fig.11 shows the Matlab/Simulink Model of Proposed Shunt Hybrid Filter with TCR Combination for Enhancing PQ features using Matlab/Simulink Platform.

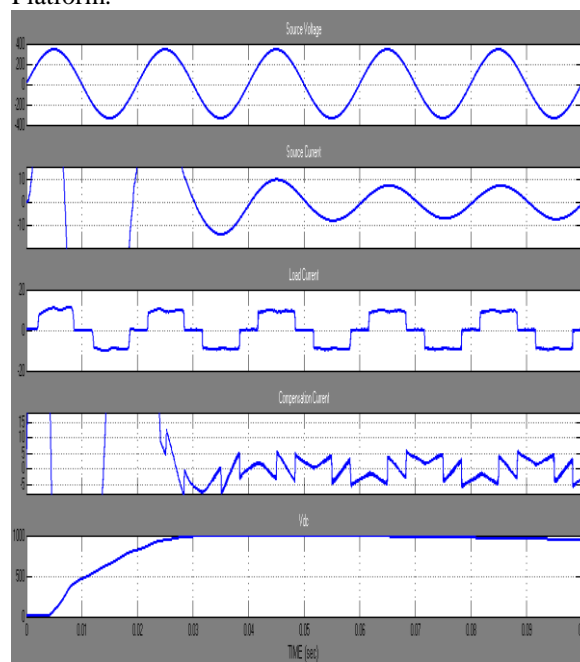


Fig.12 Source Voltage, Source Current, Load Current, Compensation Current, DC Link Voltage.

Fig.12 shows the Steady State Response of Source Voltage, Source Current, Load Current, Compensation Current, DC Link Voltage of the SHPF-TCR Compensator on Harmonic Generation Load Operated under PI Controller.

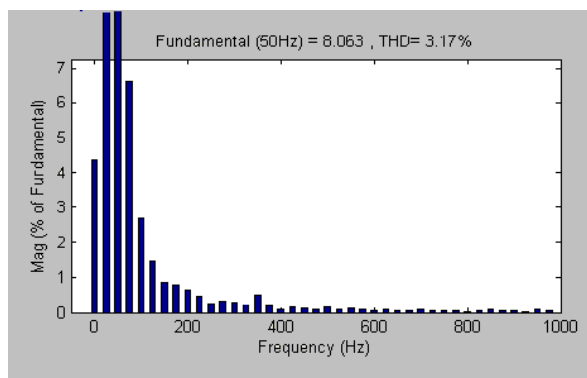


Fig.13 FFT Analysis of Source Current

Fig.13 FFT Analysis of Source Current of the SHPF-TCR Compensator on Harmonic Generation Load, attain THD as 3.17%, Operated under PI Controller.

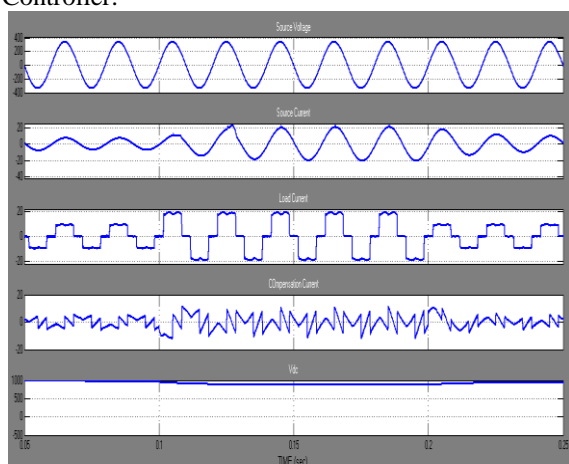


Fig.14: Source Voltage, Source Current, Load Current, Compensation Current, DC Link Voltage

Fig.14 shows the Transient Response of Source Voltage, Source Current, Load Current, Compensation Current, DC Link Voltage of the SHPF-TCR Compensator on Harmonic Generation Load Operated under PI Controller.

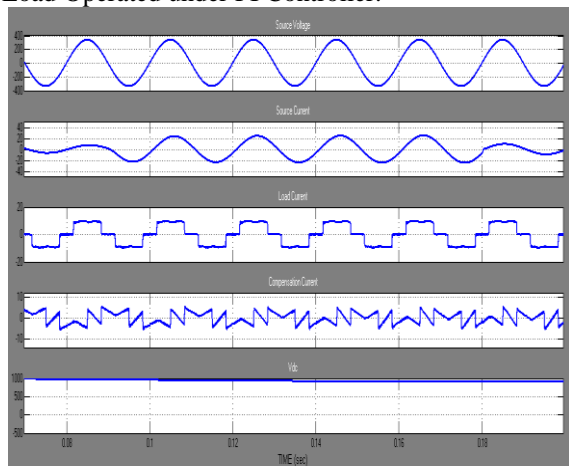


Fig.15: Source Voltage, Source Current, Load Current, Compensation Current, DC Link Voltage

Fig.15 shows the Source Voltage, Source Current, Load Current, Compensation Current, DC Link Voltage of the Dynamic response of SHPF-TCR compensator under the harmonic and reactive power type of loads Operated under PI Controller.

Case 2: Proposed Hybrid Power Filter Operated under Fuzzy Controller.

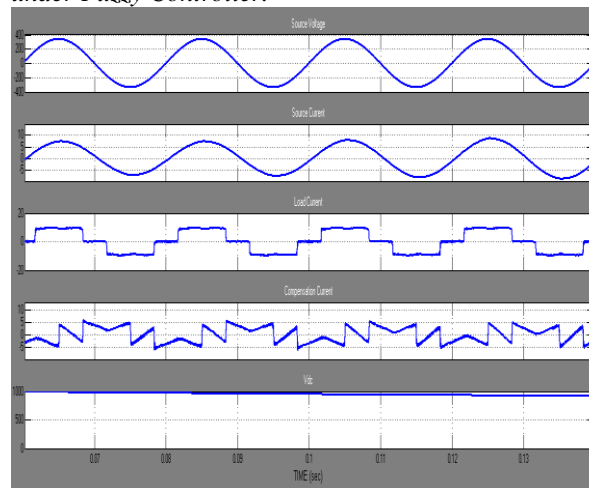


Fig.16: Source Voltage, Source Current, Load Current, Compensation Current, DC Link Voltage.

Fig.16 shows the Steady State Response of Source Voltage, Source Current, Load Current, Compensation Current, DC Link Voltage of the SHPF-TCR Compensator on Harmonic Generation Load Operated under Fuzzy Controller.

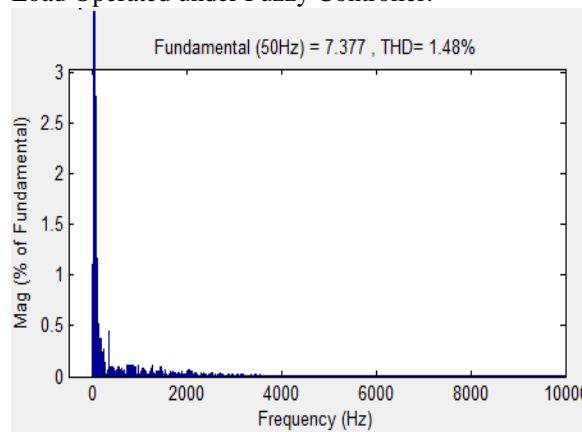


Fig.17: FFT Analysis of Source Current

Fig.17 FFT Analysis of Source Current of the SHPF-TCR Compensator on Harmonic Generation Load attains THD as 1.48%, Operated under Fuzzy Controller.

VI. CONCLUSION

A fuzzy logic HAPF controller has been designed for stabilization of power systems. The control has been tested on several load conditions with transient/dynamic/steady state conditions. The transient response of the power system with the

proposed fuzzy controller has been compared with a conventional PI control design. In this paper, an Intelligent based SHPF-TCR compensator of a TCR and a SHPF has been proposed to achieve harmonic elimination and reactive power compensation. A proposed nonlinear control scheme of a SHPF-TCR compensator has been established, simulated, and implemented by using the Matlab/Simulink platform. The shunt active filter and SPF have a complementary function to improve the performance of filtering and to reduce the power rating requirements of an active filter. It has been found that the SHPF-TCR compensator can effectively eliminate current harmonic and reactive power compensation during steady and transient operating conditions for a variety of loads. It has been shown that the system has a fast dynamic response, has good performance in both steady-state and transient operations, and is able to reduce the THD of supply currents well below the limit of 5% of the IEEE-519 standard.

REFERENCES

- [1] P. Flores, J. Dixon, M. Ortuzar, R. Carmi, P. Barriuso, and L. Moran, "Static Var compensator and active power filter with power injection capability, using 27-level inverters and photovoltaic cells," *IEEE Trans. Ind. Electron.*, vol. 56, no. 1, pp. 130–138, Jan. 2009.
- [2] H. Hu, W. Shi, Y. Lu, and Y. Xing, "Design considerations for DSP controlled 400 Hz shunt active power filter in an aircraft power system," *IEEE Trans. Ind. Electron.*, vol. 59, no. 9, pp. 3624–3634, Sep. 2012.
- [3] M. Angulo, D. A. Ruiz-Caballero, J. Lago, M. L. Heldwein, and S. A. Mussa, "Active power filter control strategy with implicit closed loop current control and resonant controller," *IEEE Trans. Ind. Electron.*, vol. 60, no. 7, pp. 2721–2730, Jul. 2013.
- [4] A. Hamadi, S. Rahmani, and K. Al-Haddad, "A hybrid passive filter configuration for VAR control and harmonic compensation," *IEEE Trans. Ind. Electron.*, vol. 57, no. 7, pp. 2419–2434, Jul. 2010.
- [5] X. Du, L. Zhou, H. Lu, and H.-M. Tai, "DC link active power filter For three-phase diode rectifier," *IEEE Trans. Ind. Electron.*, vol. 59, no. 3, pp. 1430–1442, Mar. 2012.
- [6] Z. Chen, Y. Luo, and M. Chen, "Control and performance of a cascaded shunt active power filter for aircraft electric power system," *IEEE Trans. Ind. Electron.*, vol. 59, no. 9, pp. 3614–3623, Sep. 2012.
- [7] J. A. Munoz, J. R. Espinoza, C. R. Baier, L. A. Moran, E. E. Espinosa, P. E. Melin, and D. G. Sbarbaro, "Design of a discrete-time linear control strategy for a multicell UPQC," *IEEE Trans. Ind. Electron.*, vol. 59, no. 10, pp. 3797–3807, Oct. 2012.
- [8] Y. Tang, P. C. Loh, P. Wang, F. H. Choo, F. Gao, and F. Blaabjerg, "Generalized design of high performance shunt active power filter with output LCL filter," *IEEE Trans. Ind. Electron.*, vol. 59, no. 3, pp. 1443–1452, Mar. 2012.
- [9] L. Junyi, P. Zanchetta, M. Degano, and E. Lavopa, "Control design and implementation for high performance shunt active filters in aircraft power grids," *IEEE Trans. Ind. Electron.*, vol. 59, no. 9, pp. 3604–3613, Sep. 2012.
- [10] X. Wang, F. Zhuo, J. Li, L. Wang, and S. Ni, "Modeling and control of dual-stage high-power multifunctional PV system in $d-q-0$ coordinate," *IEEE Trans. Ind. Electron.*, vol. 60, no. 4, pp. 1556–1570, Apr. 2013.
- [11] C. S. Lam, W. H. Choi, M. C. Wong, and Y. D. Han, "Adaptive dc-link voltage-controlled hybrid active power filters for reactive power compensation," *IEEE Trans. Power Electron.*, vol. 27, no. 4, pp. 1758–1772, Apr. 2012.
- [12] A. Bhattacharya, C. Chakraborty, and S. Bhattacharya, "Parallel connected shunt hybrid active power filters operating at different switching frequencies for improved performance," *IEEE Trans. Ind. Electron.*, vol. 59, no. 11, pp. 4007–4019, Nov. 2012.
- [13] S. Rahmani, A. Hamadi, K. Al-Haddad, and A. I. Alolah, "A DSP-based implementation of an instantaneous current control for a three-phase shunt hybrid power filter," *J. Math. Comput. Simul.—Model. Simul. Elect. Mach., Convert. Syst.*, vol. 91, pp. 229–248, May 2013.
- [14] A. Hamadi, S. Rahmani, and K. Al-Haddad, "Digital control of hybrid power filter adopting nonlinear control approach," *IEEE Trans. Ind. Informat.*, to be published.
- [15] A. Luo, X. Xu, L. Fang, H. Fang, J. Wu, and C. Wu, "Feedback feedforward PI-type iterative learning control strategy for hybrid active power filter with injection circuit," *IEEE Trans. Ind. Electron.*, vol. 57, no. 11, pp. 3767–3779, Nov. 2010.
- [16] S. Rahmani, A. Hamadi, N. Mendalek, and K. Al-Haddad, "A new control technique for three-phase shunt hybrid power filter," *IEEE Trans. Ind. Electron.*, vol. 56, no. 8, pp. 2904–2915, Aug. 2009.
- [17] S. Rahmani, A. Hamadi, and K. Al-Haddad, "A Lyapunov-function-based control for a three-phase shunt hybrid active filter," *IEEE*

- Trans. Ind. Electron.*, vol. 59, no. 3, pp. 1418–1429, Mar. 2012.
- [18] C. A. Silva, L. A. Cordova, P. Lezana, and L. Empringham, “Implementation and control of a hybrid multilevel converter with floating dc links for current waveform improvement,” *IEEE Trans. Ind. Electron.*, vol. 58, no. 6, pp. 2304–2312, Jun. 2011.
- [19] M. I. Milanés-Montero, E. Romero-Cadaval, and F. Barrero-González, “Hybrid multiconverter conditioner topology for high-power applications,” *IEEE Trans. Ind. Electron.*, vol. 58, no. 6, pp. 2283–2292, Jun. 2011.
- [20] A. Luo, S. Peng, C. Wu, J. Wu, and Z. Shuai, “Power electronic hybrid system for load balancing compensation and frequency-selective harmonic suppression,” *IEEE Trans. Ind. Electron.*, vol. 59, no. 2, pp. 723–732, Feb. 2012.
- [21] A. Luo, Z. Shuai, W. Zhu, and Z. John Shen, “Combined system for harmonic suppression and reactive power compensation,” *IEEE Trans. Ind. Electron.*, vol. 56, no. 2, pp. 418–428, Feb. 2009.